

HUMAN-CENTERED
COMPUTING

Holistic Sensing and Active Displays for Intelligent Driver Support Systems

Mohan M. Trivedi and Shinko Y. Cheng
University of California, San Diego

A multidisciplinary research effort at UCSD focuses on the design, development, and evaluation of novel computational frameworks for vehicle-based safety systems. The dynamic active display presents visual alerts to the driver based on the surrounding environment, vehicle dynamics, and driver's state as well as a driver-intent analysis and situational awareness system.

The automobile has radically transformed how we live and work, providing people around the world with unprecedented mobility. However, despite their many benefits, motor vehicles pose a considerable safety risk. According to the World Health Organization, traffic collisions account for an estimated 1.2 million fatalities and up to 50 million injuries worldwide each year (www.who.int/world-health-day/2004/infomaterials/world_report/en).

Most roadway accidents are caused by driver error. A 2006 study sponsored by the US Department of Transportation's National Highway Traffic Safety Administration concluded that driver inattention contributes to nearly 80 percent of crashes and 65 percent of near crashes (www-nrd.nhtsa.dot.gov/departments/nrd-13/810594/images/810594.pdf).

Embedded computing systems are increasingly used in today's vehicles to make them safer as well as more reliable, comfortable, and enjoyable to drive. However, to be effective, such technologies must be human-centric—they must incorporate an understanding of both general driver behavior and the vehicle operator's unique driving characteristics. These technologies also must be introduced carefully to ensure that they do not confuse or distract the driver, thereby undermining their intended purpose.

The Laboratory for Intelligent and Safe Automobiles (<http://cvrr.ucsd.edu/LISA>) at the University of California,

San Diego, brings together researchers from a wide range of disciplines to design, develop, and evaluate intelligent driver-support systems (IDSSs). LISA project participants share their expertise as well as both testbeds and analysis visualization tools, producing contributions and raising new research questions that would not have emerged if each group worked independently.

These multidisciplinary efforts have led to the creation of novel instrumented vehicles that capture rich contextual information about the environment, vehicle, and driver (EVD) as well as realistic data for developing better algorithms to analyze multisensory input. A promising technology to emerge from this work is the *dynamic active display*, an IDSS that projects safety-critical warnings based on EVD data as well as in response to a unique driver-intent analysis and situational awareness system onto a windshield-size heads-up display.

HUMAN-CENTERED ACTIVE SAFETY

Vehicle-based safety systems generally fall into one of two categories. *Passive* safety systems such as seat belts, airbags, collapsible steering columns, and shatter-resistant windshields are designed to reduce the risk or severity of injuries sustained in collisions, and require minimal knowledge of the vehicle's overall state. In contrast, *active* safety systems aim to prevent vehicular accidents. Example systems include antilock brakes, traction control systems, and electronic stability control systems,

all of which interpret signals from several sensors to help the driver maintain vehicular control.

Preventing a collision is obviously more desirable, but active safety systems pose considerable design challenges. One of these is accurately, reliably, and efficiently identifying the conditions that would lead to a crash, and then forcing corrective actions to prevent it. Another is determining what, if any, actions the driver has taken in response to the impending collision.

As Figure 1 shows, a vehicle-based active safety system has three main parts. The *sensing* subsystem captures the dynamic EVD state conditions and sends a description of these to the *analysis* subsystem, which uses a model-based approach to compute some measure of safety underlying those particular conditions. If this measure falls under a predefined threshold, the analysis module directs the *safety-control* subsystem to initiate a corrective course of action so that the vehicle can always operate within safe margins.

The primary task of a vehicle-based active safety system is to help the driver make stress-free corrective decisions in the face of potentially dangerous and continually changing EVD conditions. Accomplishing this requires resolving numerous complex research questions, including:

- What constitutes situational awareness of the system?
- What computational framework will ensure a robust system?
- How does the system measure situational criticality?
- How does the system measure driver state and intentions?
- When and how does the system warn the driver to ensure proper course corrections?

These questions invite input from other disciplines besides computer science and engineering including psychology, cognitive science, decision theory, and ethnography. Although human-centric scientific studies have been gaining acceptance in intelligent system design, they typically remain at an anecdotal or case-study level, making it difficult to extrapolate results to larger populations. On the other hand, while simulator-based design efforts have produced good generalizable results, they are

too simplistic to capture the richness of real-life driving situations.

HOLISTIC SENSING

Designing an effective IDSS requires understanding how different types of how drivers make decisions in various circumstances. This can only be obtained by conducting real-world studies that dynamically capture synchronized EVD data and using analytical tools to explore how these EVD elements interact in a holistic manner. Figure 2 shows a framework for a multifunctional, active computer-vision-based dynamic concept-capture system.

We used the LISA-P and LISA-Q intelligent vehicle testbeds to observe numerous drivers in a naturalistic state. These testbeds incorporate a wide range of sensors to capture the complete driving context—the

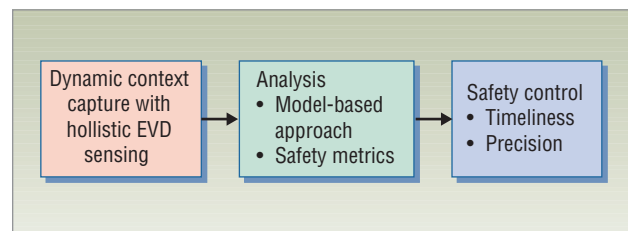


Figure 1. A vehicle-based active safety system contains sensing, analysis, and safety-control modules.

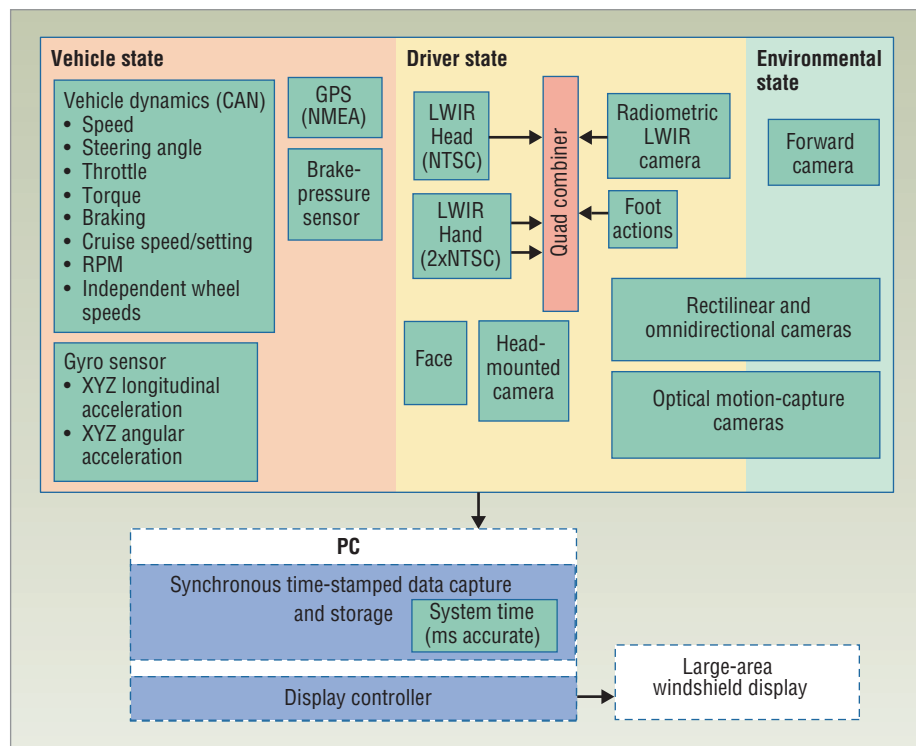


Figure 2. Dynamic concept-capture system. The multifunctional, active computer-vision-based system captures synchronized data about the environment, vehicle, and driver and analyzes how these EVD elements interact in a holistic manner.

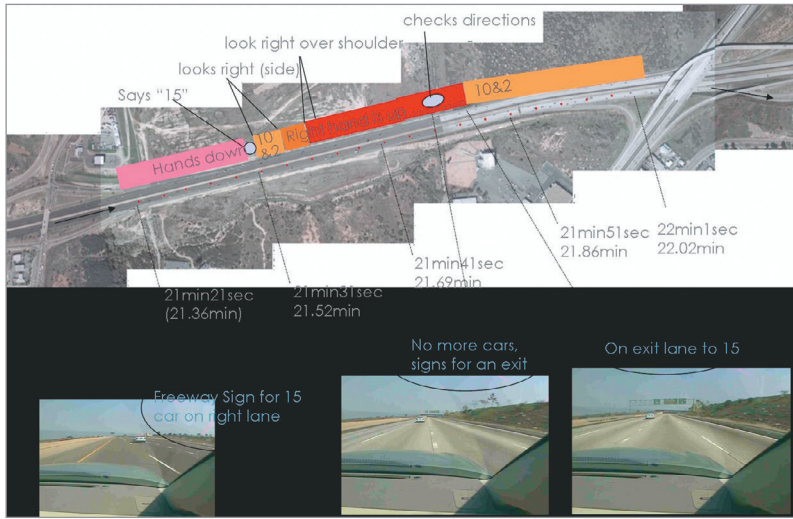


Figure 3. Driver behavior analysis. LISA testbeds provide rich data to examine drivers' actions over time and uncover meaningful categories of driving situations—in this case, lane changing—with corresponding information needs and behavioral sequences.

surrounding environment, vehicle performance, and driver actions—during the entire course of a trial.

Digital video streams provide data on the vehicle's environment using forward, rear, and side-viewing rectilinear cameras and a 360-degree omnidirectional camera. A long-

wavelength infrared camera (LWIR) captures the driver's hands and face, a near-IR camera with IR illuminators records the driver's foot actions, a camera facing the driver captures the driver's face and hand movements, and a headband-mounted camera records the driver's point of view.

An x86-processor-based computer located in the vehicle's rear captures, compresses (using external hardware), and time-stamps all of these DV streams in real time. A controller area network (CAN) bus integrates vehicle state information, including speed, engine rpm, steering angle, and throttle and brake pressure. A GPS device tracks vehicle location.

An optical motion-capture system simultaneously measures the driver's body posture and hand positions while driving. This system provides groundtruth for marker-less vision-based algorithms to measure the driver's gaze origin and direction. It also

captures pristine data for analysis to determine the extent to which an automated system can use body-posture information to recognize and predict driving behavior.¹

As Figure 3 shows, these testbeds provide rich data that we have used to analyze drivers' behavior over time

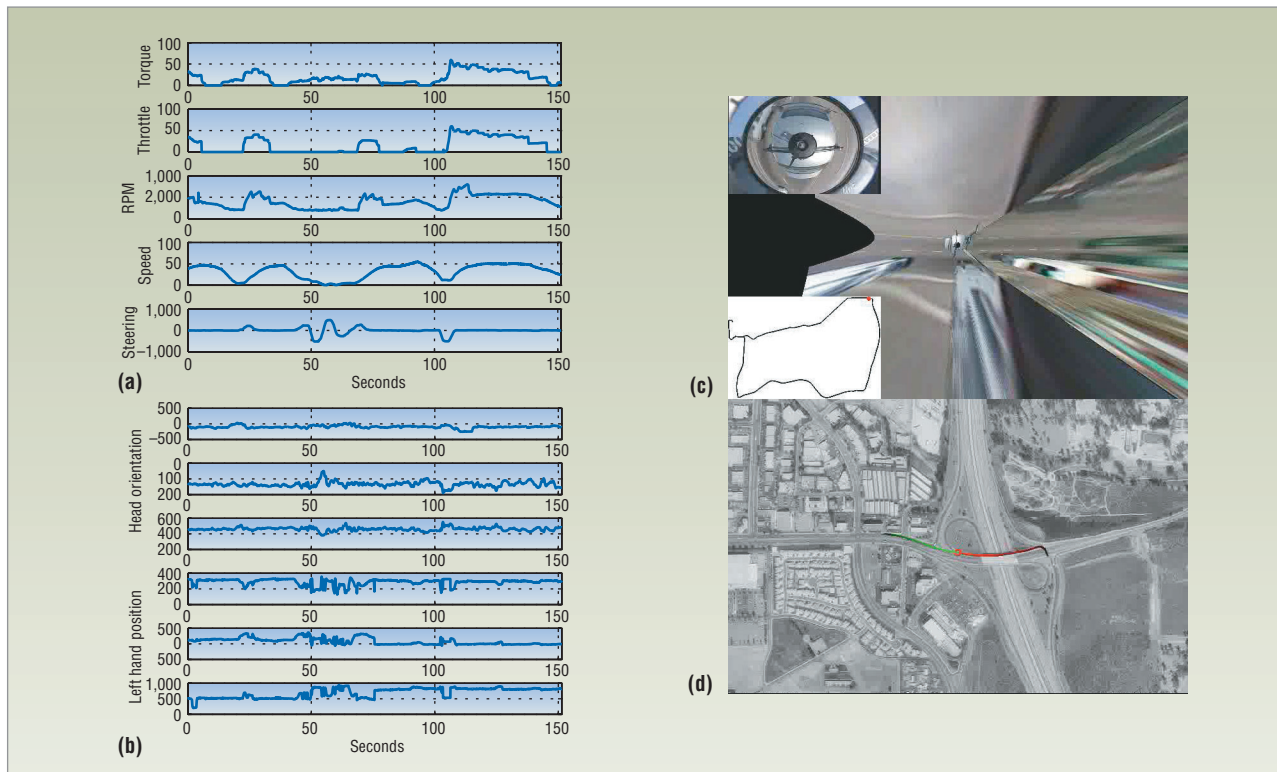


Figure 4. Representing the complete driving context. Data postprocessing tools integrate the LISA testbeds' various video, audio, and sensor streams, including (a) CAN data and (b) motion-capture data, to generate (c) an environmental map and (d) an aerial view of the vehicle's location.

and uncover meaningful categories of driving situations, such as lane changing, with corresponding information needs and behavioral sequences.²

We have also developed several data postprocessing tools that integrate the testbeds' various video, audio, and sensor streams to capture the complete driving context in different scenarios. As Figure 4 shows, these tools can be used to generate, among other things, an environmental map (based on an inverse projection of the cameras) and an aerial view of the vehicle's location.³

DYNAMIC ACTIVE DISPLAY

Building on its fine-grained studies of driving behavior and systems used to collect and analyze EVD data, LISA is developing the dynamic active display, a novel IDSS that actively helps drivers make corrective actions by projecting visual warnings about roadway hazards based on the driver's body posture, awareness level, and anticipated intentions as well as vehicle state. As Figure 5 shows, the DAD consists of a multifunctional integrated imaging and sensor array, a driver-intent analysis and situational-awareness system, and a windshield-size heads-up display (HUD).

The sensory array collects input from various EVD sensors to obtain data about vehicle dynamics, the driving environment, and the driver's head orientation, eye location, and hand positions. The driver-intent analysis and situational-awareness system processes information about the driver's state and situation criticality to determine what, where, and when to display appropriate

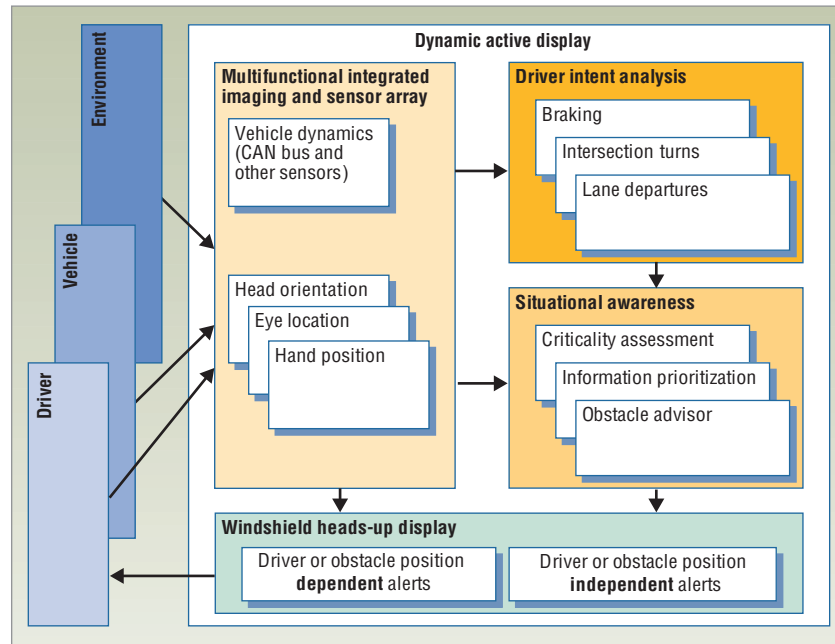


Figure 5. Dynamic active display framework. The DAD consists of a multifunctional integrated imaging and sensor array, a driver-intent analysis and situational awareness system, and a windshield-size heads-up display.

warnings. Use of a HUD rather than a conventional heads-down display minimizes the time required to look away from the road and reduces the need for reaccommodation of focus, an issue of increasing importance for drivers as they age. Studies have shown that HUDs save from 0.8 to 1 second in driver reaction time over HDDs when displaying vehicle warning information.⁴

Researchers have experimented with many types of HUDs in automobiles.^{5,6} As Figure 6a shows, the HUD in the DAD system has a uniquely large field of view spanning the entire windshield (approximately 67

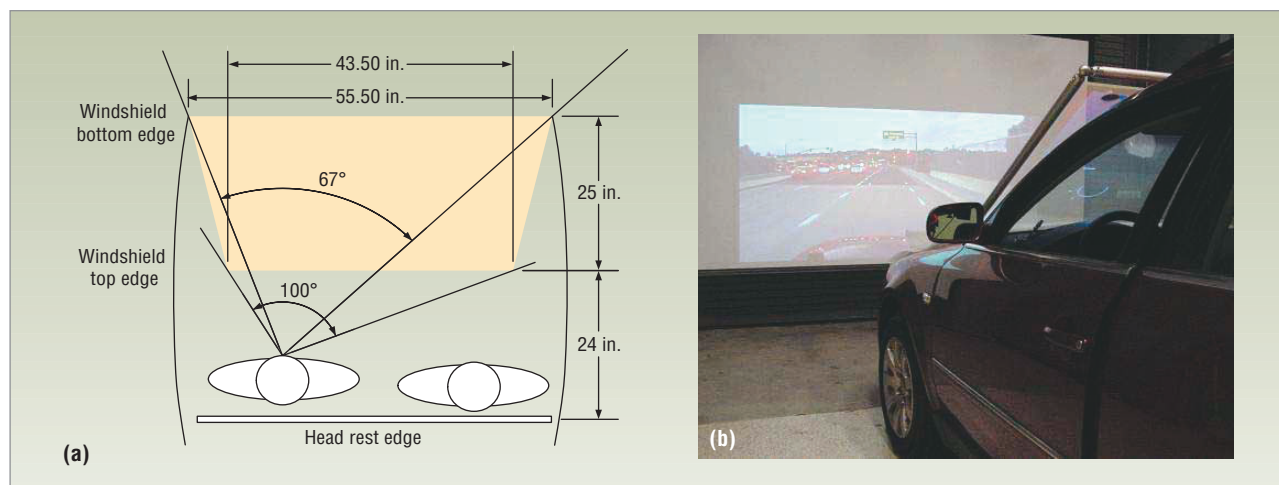


Figure 6. DAD heads-up display. (a) The HUD's field of view spans the entire windshield. (b) Experimental setup showing the HUD's highly transparent display screen and a second nontransparent display screen positioned in front of the vehicle showing video of a drive from the operator's point of view. HUD display screen courtesy of J.C. Morgan, ProScreen.

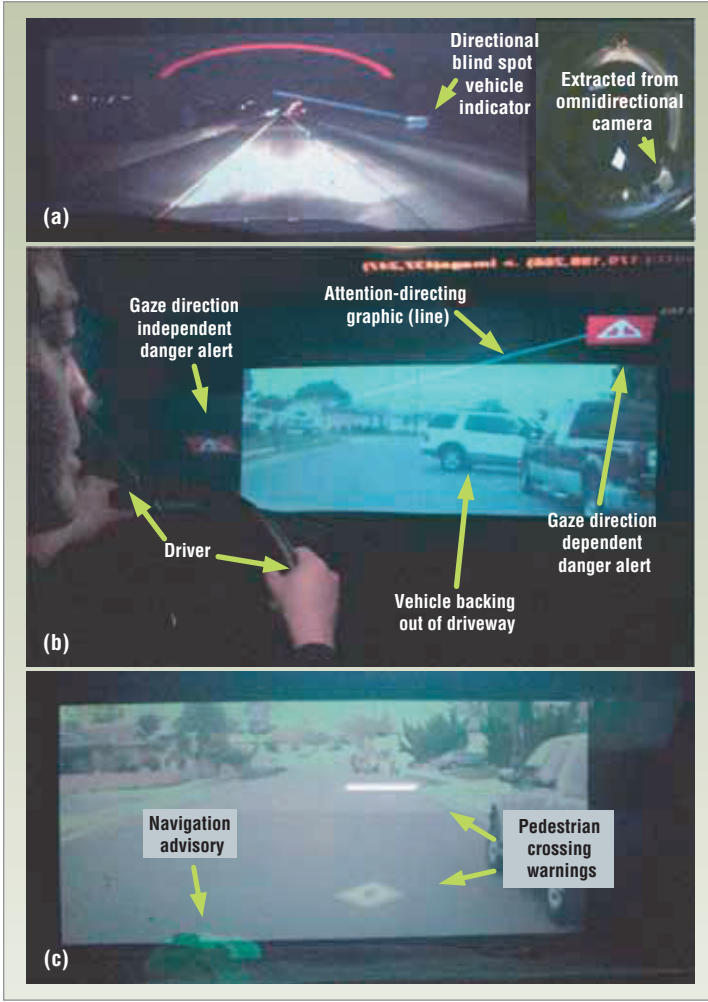


Figure 7. DAD display modes. The system projects safety-critical warnings (a) in a constant single location, (b) at or near the driver's line of sight, and (c) on top of obstacles as perceived by the driver.

degrees for the bottom edge to 100 degrees for the top edge). In our experimental HUD setup, shown in Figure 6b, we position a highly transparent acrylic screen made specifically for laser projectors over the test vehicle's windshield; a second nontransparent projection screen in front of the vehicle shows video of a drive through city streets and on freeways from the driver's point of view.

The DAD projects safety-critical warnings in three ways:

- in a constant single location,
- at or near the driver's line of sight, and
- on top of obstacles as perceived by the driver.

Displaying alerts in a constant location is trivial. However, the other two display modes provide a level of danger localization previously achieved only in fighter planes.

Projecting a graphic along the driver's line of sight requires a description of the driver's gaze origin \mathbf{o} and

direction \mathbf{d} , which are extrapolated from motion-capture video of the driver's head orientation and the windshield's surface geometry. We represent gaze as the vector (\mathbf{o}, \mathbf{d}) , where $\mathbf{o} = (x, y, z)^T$ and $\mathbf{d} = (dx, dy, dz)$, with $\|\mathbf{d}\| = 1$; this represents five degrees of freedom. In the same coordinate space as the driver's head, the display surface's geometry can be described as

$$w(\mathbf{p}) = 0 \quad (1)$$

where $\mathbf{p} = (x, y, z)^T$ is a point in R^3 space. Any point that satisfies this equation lies on the windshield in this coordinate space. Finally, the potentially nonlinear function $f: R^3 \rightarrow R^2$ transforms points on the windshield \mathbf{p} in 3D coordinates to points on the display \mathbf{u} in 2D coordinates:

$$\mathbf{u} = f(\mathbf{p}) \quad (2)$$

This function can be constructed by assuming a distortion model from a perfect plane or via a table lookup and piecewise linear interpolation relating windshield points to display coordinates.

The problem is to find the point \mathbf{p}^* on the line formed by the gaze that intersects the windshield—that is, a point that satisfies Equation 1—and the corresponding point in display coordinates \mathbf{u}^* , obtained using Equation 2. We assume for now that the windshield is perfectly planar with a surface normal \mathbf{n} and origin \mathbf{w}_o . The windshield surface equation can then be given by

$$w_{\text{planar}}(\mathbf{p}) = \begin{bmatrix} \mathbf{n} \\ -\mathbf{n}^T \mathbf{w}_o \end{bmatrix}^T \begin{bmatrix} \mathbf{p} \\ 1 \end{bmatrix} = 0 \quad (3)$$

The points along the line formed by the driver's gaze are given by

$$\mathbf{p} = \mathbf{o} + \mu \mathbf{d} \quad \forall \mu \in \mathbb{R} \quad (4)$$

where μ describes the location of point \mathbf{p} as a proportion of $\|\mathbf{d}\|$ along the \mathbf{d} direction from \mathbf{o} . The point \mathbf{p}^* that lies on the windshield plane can be found by combining Equations 3 and 4:

$$\mathbf{p}^* = \mathbf{o} + \left(\frac{\mathbf{n}^T \mathbf{w}_o - \mathbf{n}^T \mathbf{o}}{\mathbf{n}^T \mathbf{d}} \right) \mathbf{d} \quad (5)$$

Because of our planar assumption, the transformation function f is given by

$$\mathbf{u}^* = \mathbf{K} \mathbf{R} \mathbf{p}^* = \begin{bmatrix} \mathbf{a} & 0 & 0 \\ 0 & \mathbf{b} & 0 \end{bmatrix} \begin{bmatrix} \mathbf{x} & \mathbf{y} & (\mathbf{x} \times \mathbf{y}) \end{bmatrix} \mathbf{p}^* \quad (6)$$

where x and y are the local x - and y -axes of the windshield plane, and a and b are the scaling factors across these axes to translate physical coordinates to display coordinates.

Overlaying alerts on top of objects ahead of the vehicle requires knowledge of the driver's head orientation o , the object's position q , the windshield surface geometry $w(p) = 0$, and a windshield transformation function f . Object position is obtained by annotating motion-capture video of object locations in the image frame and determining the corresponding location on the forward projection screen. The intersection point p^* between the windshield surface and the line formed between o and q is the point on the windshield (in physical coordinates) that lies directly over the driver's view of the object. The transformed point $u^* = f(p^*)$ is the corresponding point in display coordinates.

Figure 7 illustrates the three DAD modes in our simulator. Figure 7a shows a static visual alert indicating the presence of a vehicle in the driver's right-side blind spot, projected on the HUD so that the driver can maintain peripheral sight of the road ahead. In Figure 7b, the system uses an attention-getting line and icons to direct the driver, who is originally looking ahead, to shift his gaze to the right to notice a vehicle backing out of a driveway. In Figure 7c, overlay graphics call out roadway markings and a pedestrian ahead.

HAND TRACKING FOR DRIVER INTENT

Although graphic alerts significantly improve response time, they also compete for the driver's limited visual attention—unlike audible alerts, which people process almost independently of visual recognition tasks.^{7,8} In many situations, projecting warning icons might actually increase the risk of a collision. For example, when turning at an intersection, a driver must be mindful of traffic controls, staying within the turning lane, other vehicles and pedestrians, and maintaining a safe speed and distance from other vehicles while accelerating into the turn. Projecting an alert about, say, a pedestrian crossing the street that the driver has already seen and slowed down for can distract the driver from other important tasks.

To address this problem, the DAD anticipates driver actions and provides advisory information specific to a maneuver; it can also refrain from displaying alerts if the driver is aware of obstacles ahead. The system uses driver intent as a means of determining awareness of

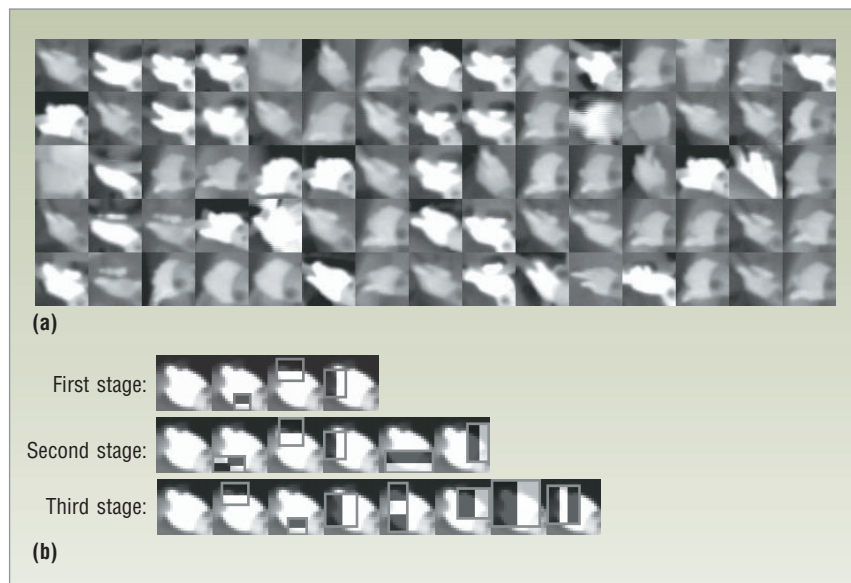


Figure 8. Extracting driver hand positions from LWIR images. (a) Positive example LWIR images of drivers' hands. (b) Features used in the first three stages of the classifier cascade for hand detection.

potential roadway hazards. If the driver intends to perform a maneuver in the presence of a danger, the DAD concludes that the driver is unaware of that danger.

Previous LISA research demonstrated that driver lane-change and turn intent can be extrapolated from EVD data, particularly data relating to driver posture. To determine lane-change intent, we extracted head-motion and lane-position information from video taken by various cameras placed around a test vehicle.³ In addition, we achieved a 90 percent success rate using marker-based motion-capture video of driver hand position, head orientation, and other cues to predict turn intent at the moment a vehicle enters an intersection.^{1,9} The next step was to devise a method of visually tracking hand position and determining steering-wheel grasp type without the need for markers.

Detecting and tracking hand position

Our proposed approach utilizes LWIR cameras' heat-sensing capability to track driver hand movement. This attribute is especially useful inside a vehicle where visible illumination constantly changes and skin temperature hovers at a relatively constant value. As Figure 8a shows, we extract 20×20 pixel positive sample thermal images of driver hand locations using a popular object detector that combines Haar-like features with a boosted cascade of weak stump classifiers. Figure 8b shows the most salient features chosen in the first three stages of the classifier cascade.

The process usually detects two but occasionally detects more than two, one, or no candidate image regions as hands. To discern which detected candidates are truly hands and which among these are the left and

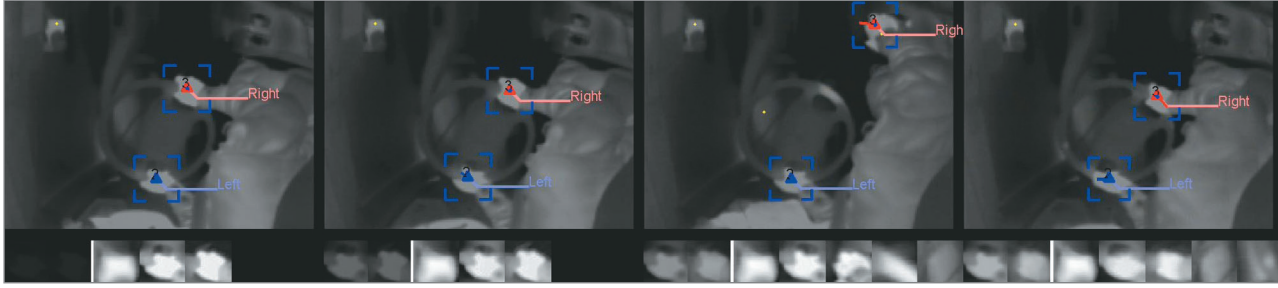


Figure 9. Tracking driver hand position. Tracking results show left and right hand association (top) and the corresponding stored appearance models (below) of the hands.

right hands, we track all hand targets using a constant-velocity Kalman filter with probabilistic data association. We classify the most likely targets as a left or right hand by examining the

- probability that either hand is present on either side of the steering wheel;
- similarity of the target's appearance with that of the last recognized left or right hand target; and
- longevity or confidence of the track, a likelihood ratio comparing the probability that the measurement belonged to the Poisson distributed background or the valid next measurement from a track.

All tracked targets maintain an adaptive appearance model $T_i \in \mathbb{R}^{M \times M}$, which is an autoregressive average of all image patches of all measurements. Potential and valid targets also accumulate a left-hand and right-hand

likelihood measure that consists of two quantities: a target's proximity to the left or right hand's usual position in the driver's area, and the similarity in appearance of the target's appearance model with the stored left- and right-hand appearances U_L and U_R .

The first quantity is modeled as a bivariate Gaussian probability, with log likelihood values for the left and right hand given by $l_{i,p} = \log(\mathbf{x}_i | \mu_L, \Sigma_L)$ and $r_{i,p} = \log(P(\mathbf{x}_i | \mu_R, \Sigma_R))$, where $\mu_L, \mu_R \in \mathbb{R}^2$. The normalized sum of squared difference measures similarity of the appearance model of T_i to U_L and U_R . Together, the two quantities form a likelihood that the target is a left or a right hand:

$$l_i = \log(P(\mathbf{x}_i | \mu_L, \Sigma_L) \cdot (1 - \text{NSSD}_L))$$

$$r_i = \log(P(\mathbf{x}_i | \mu_R, \Sigma_R) \cdot (1 - \text{NSSD}_R))$$

where $\text{NSSD}_b = \|T_i - U_b\|^2 / M^2$ and $M \times M$ are the appearance model's dimensions. Amounts accumulate with a forgetting factor α_s .

A target with a higher left-hand score relative to the right-hand score indicates that it has hovered over the likely left-hand position longer than in the likely right-hand position in the image. A target with a higher left-hand score relative to all other target left-hand scores indicates a higher amount of confidence of its being the left hand. Finally, among the valid targets ($E \geq \tau_E$), those with the highest left-hand score and right-hand score are classified as the left and right hands, respectively.

Figure 9 provides an example of tracking results showing left and right hand associations and the corresponding stored appearance models (image patches) of the hands.

Determining steering-wheel grasp

While detecting and tracking hands from LWIR imagery, we also record steering-wheel angle and hand angular velocity and combine this data with knowledge of hand location to describe various grasp operation triplets.

Borrowed from linguistics, an operation triplet consists of three elements: agent, motion, and target. In this case, the agents are the left and right hands, and the target is the steering wheel. In terms of motion, each hand can

Table 1. Steering-wheel grasp operation triplets.

| Grasp operation triplet | Conditions |
|-------------------------|---|
| h Hand | $d(\mathbf{x}_h) - 1 \leq \tau_d$ |
| Grasp + No move | $\ \omega_{sw} - \omega_h\ \leq \tau_\omega$ |
| SW | $\theta_{sw} = 0$ |
| h Hand | $d(\mathbf{x}_h) - 1 \leq \tau_d$ |
| Grasp + Turn left | $\ \omega_{sw} - \omega_h\ \leq \tau_\omega$ |
| SW | $\theta_{sw} < 0$ |
| h Hand | $d(\mathbf{x}_h) - 1 \leq \tau_d$ |
| Grasp + Turn right | $\ \omega_{sw} - \omega_h\ \leq \tau_\omega$ |
| SW | $\theta_{sw} > 0$ |
| h Hand | $d(\mathbf{x}_h) - 1 \leq \tau_d$ |
| Grasp + Sliding over | $\ \omega_{sw} - \omega_h\ > \tau_\omega$ |
| SW | |
| h Hand | $d(\mathbf{x}_h) - 1 > \tau_d$ |
| Other move | |
| Null | |

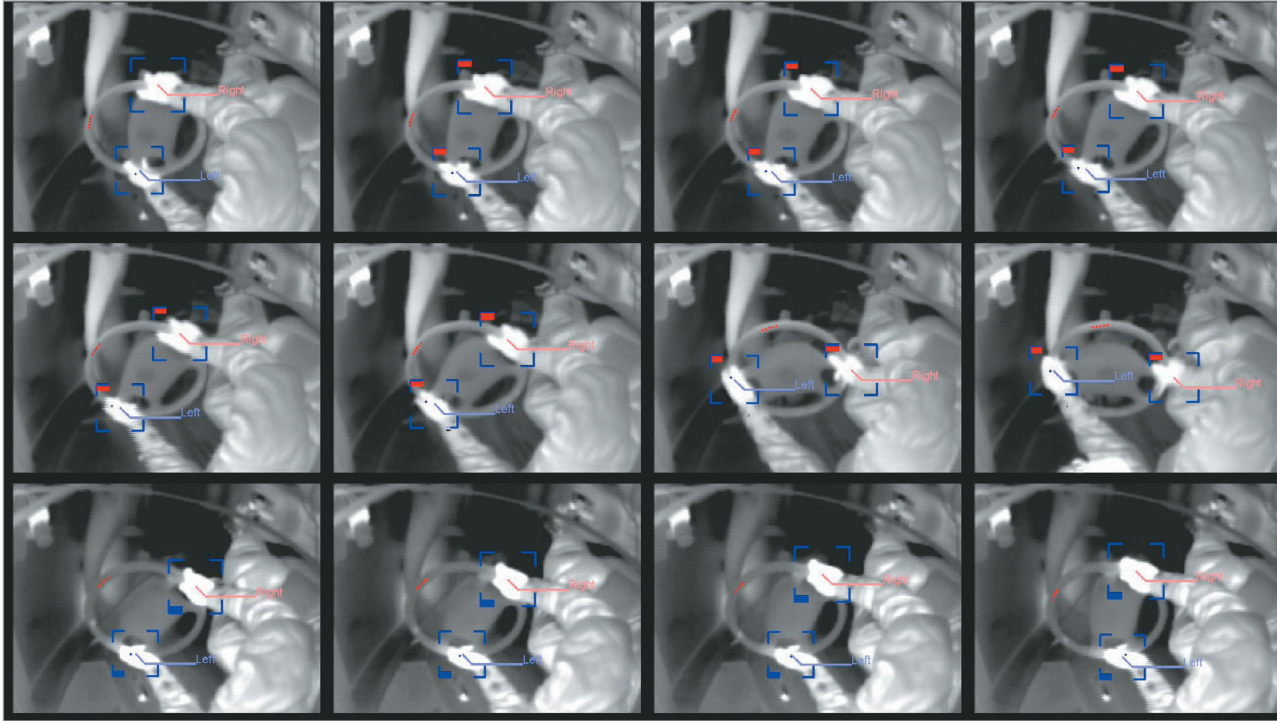


Figure 10. *Determining steering-wheel grasp operation. Grasp recognition results showing the driver grasping the wheel and moving it right and then left.*

- grasp but not move the steering wheel,
- grasp and move the steering wheel counterclockwise,
- grasp and move the steering wheel clockwise,
- grasp the steering wheel loosely and allow it to turn underneath, or
- perform some other motion toward the steering wheel.

To determine if the hand is grasping the steering wheel, we use an approximate model to measure the distance between the hand and steering wheel. We accomplish this by fitting an ellipse over the steering wheel in the image such that any point \mathbf{x} on the steering wheel in the image is a distance $d(\mathbf{x}) = 1$ away from the center of the steering wheel using the weighted 2-norm, $d(\mathbf{x}) = (\mathbf{x} - \mathbf{x}_o)^T \mathbf{S}(\mathbf{x} - \mathbf{x}_o)$ where \mathbf{x}_o is the center of the steering wheel in image coordinates.

We consider a hand detected within a certain distance from this ellipse, or $d(\mathbf{x}) < \tau_d$, to be grasping the wheel; we regard a hand beyond that distance as performing some other motion toward the wheel. To determine which of the four grasping maneuvers the hand is performing, we examine the coincidence of the steering-wheel angle and hand angular velocities. If the angular velocities between the wheel and hands exceed a threshold τ_ω , we consider the hands to be grasping the wheel loosely and allowing it to turn underneath. If the angular velocities are within that threshold, we regard the hands as holding the wheel

still, turning it clockwise, or turning it counterclockwise when the angular velocity is zero, positive, or negative, respectively.

Table 1 summarizes the conditions under which the five operation triplets occur, while Figure 10 provides an example of grasp recognition results showing the driver's hands grasping the steering wheel and moving it left and then right.

The goal of IDSSs is to prevent collisions by providing timely warnings to the driver, who must always be—at least in the foreseeable future—the final decision maker. Unlike fully autonomous vehicle systems, IDSSs like the DAD share perception, planning, and execution tasks with human operators. Designing such systems thus requires a multidisciplinary approach that goes beyond engineering and computer science to include studies of human behavior.

At LISA we continue to evaluate the DAD's effectiveness to refine its capabilities. Recent road trials indicate that projecting the vehicle's speed and the road's speed limit on the HUD can improve the driver's ability to maintain a legal speed by 40 percent.¹⁰ We continue to pursue innovative improvements in display technology, including a more robust and cost-effective means of looking in and out of vehicles, as well as multimodal warning systems comprising haptic, auditory, and visual displays. ■

Acknowledgments

We thank the Digital Media Initiative (DiMI) of the UC Discovery Program and Volkswagen-Audi for their sponsorship. We also thank our fellow researchers at LISA for their cooperation. Other UCSD colleagues provided invaluable contributions, including Jim Hollan and his team from the Distributed Cognition and Human Computer Interaction Lab, Hal Pashler and his team from the Attention and Perception Lab, Bhaskar Rao and his team from the Digital Signal Processing Lab, and David Malmberg of the Scripps Institution of Oceanography. We are likewise grateful to our industrial collaborators for their guidance and support, particularly the research teams led by Arne Stoschek, Jaime Camhi, Berkhard Huhnke, Erwin Boer, Akio Kinoshita, and Satoshi Kitazaki.

References

1. S.Y. Cheng and M.M. Trivedi, "Turn-Intent Analysis Using Body Pose for Intelligent Driver Assistance," *IEEE Pervasive Computing*, vol. 5, no. 4, 2006, pp. 28-37.
2. J.C. McCall et al., "A Collaborative Approach for Human-Centered Driving Assistance Systems," *Proc. 7th Int'l IEEE Conf. International Transportation Systems*, IEEE Press, 2004, pp. 663-667.
3. J.C. McCall and M.M. Trivedi, "Driving Behavior and Situation-Aware Brake Assistance for Intelligent Vehicles," *Proc. IEEE*, vol. 95, no. 2, 2007, pp. 374-387.
4. Y-C. Liu and M-H. Wen, "Comparison of Head-Up Display (HUD) vs. Head-Down Display (HDD): Driving Performance of Commercial Vehicle Operators in Taiwan," *Int'l J. Human-Computer Studies*, vol. 61, no. 5, 2004, pp. 679-697.
5. K.W. Gish and L. Staplin, *Human Factors Aspects of Using Head Up Displays in Automobiles: A Review of the Literature*, tech. report DOT HS 808 320, National Highway Traffic Safety Administration, US Department of Transportation, 1995; www.itsdocs.fhwa.dot.gov/jpodocs/edlbrow/3R_01!.pdf.
6. H. Watanabe et al., "The Effect of HUD Warning Location on Driver Responses," *Proc. 6th Ann. World Congress on Intelligent Transportation Systems*, ITS America, 1999, pp. 1-10; www.umich.edu/~driving/publications/ITS-Watanabe1999.pdf.
7. G. Johannsen, "Auditory Displays in Human-Machine Interfaces," *Proc. IEEE*, vol. 92, no. 4, 2004, pp. 742-758.
8. J. Levy, H. Pashler, and E. Boer, "Central Interference in Driving: Is There Any Stopping the Psychological Refractory Period?," *Psychological Science*, vol. 17, no. 3, 2006, pp. 228-235.
9. S.Y. Cheng, S. Park, and M.M. Trivedi, "Multi-Spectral and Multi-Perspective Video Arrays for Driver Body Tracking and Activity Analysis," to appear in *Computer Vision and Image Understanding*, special issue on advances in vision algorithms and systems beyond the visible spectrum, 2007.
10. S.Y. Cheng, A. Doshi, and M.M. Trivedi, "Active Heads-Up Display Based Speed Compliance Aid for Driver Assistance: A Novel Interface and Comparative Experimental Studies," to appear in *Proc. 2007 IEEE Intelligent Vehicles Symp.*, IEEE Press, 2007.

Get access

to individual
IEEE Computer Society
documents online.

More than 100,000 articles and
conference
papers available!

\$9US per article for members

\$19US for nonmembers

[www.computer.org/
publications/dlib](http://www.computer.org/publications/dlib)

IEEE
computer
society

Mohan M. Trivedi is a professor in the Department of Electrical and Computer Engineering and founding director of the Computer Vision and Robotics Research Laboratory at the University of California, San Diego. His research interests include computer vision, intelligent vehicles and transportation systems, and human-machine interfaces. Trivedi received a PhD in electrical engineering from Utah State University. He is a member of the IEEE Computer Society, from which he received both the Pioneer Award and the Meritorious Service Award, and a Fellow of the International Society for Optical Engineering. Contact him at mtrivedi@ucsd.edu.

Shinko Y. Cheng is a PhD candidate in the Department of Electrical and Computer Engineering as well as a member of the Computer Vision and Robotics Research Laboratory at the University of California, San Diego. His research interests include computer vision systems, machine learning, and intelligent vehicles. Cheng is a student member of the IEEE Computer Society. Contact him at sycheng@ucsd.edu.